Persistent spin dynamics in magnetically ordered honeycomb-lattice cobalt oxides

Ping Miao,[1,2,*] Xianghong Jin,[3] Weiliang Yao,[3] Yue Chen,[3] Akihiro Koda,[4,5] Zhenhong Tan,[1,2] Wu Xie,[1,2] Wenhai Ji,[1,2] Takashi Kamiyama,[1,2] and Yuan Li[3,†]

[1]*Institute of High-Energy Physics, Chinese Academy of Sciences, Beijing 100049, China*
[2]*Spallation Neutron Source Science Center, Dongguan 523803, China*
[3]*International Center for Quantum Materials, School of Physics, Peking University, Beijing 100871, China*
[4]*Institute of Materials Structure Science, High Energy Accelerator Research Organization (KEK), Tokai, Ibaraki 319-1106, Japan*
[5]*Department of Materials Structure Science, Sokendai (The Graduate University for Advanced Studies), Tokai, Ibaraki 319-1106, Japan*

(Received 15 August 2023; revised 14 March 2024; accepted 1 April 2024; published 22 April 2024)

In the quest to find quantum spin liquids, layered cobalt oxides $Na_2Co_2TeO_6$ and $Na_3Co_2SbO_6$ have been proposed as promising candidates for approximating the Kitaev honeycomb-lattice model. Yet, their suitability has been thrown into question due to observed long-range magnetic order at low temperatures and indications of easy-plane, rather than Kitaev-type, spin anisotropy. Here, we use muon-spin relaxation to reveal an unexpected picture: Contrary to the anticipated static nature of the long-range order, the systems show prevalent spin dynamics with a spatially uneven distribution and varied correlation times. This underlines that the magnetic ground states cannot be solely described by the long-range order, suggesting a significant role of quantum fluctuations. Our findings not only shed light on the complex physics of these systems but also underscore the need for a refined approach in the search for realizable quantum spin liquids.

DOI: 10.1103/PhysRevB.109.134431

I. INTRODUCTION

Materials that might realize the Kitaev model for quantum spin liquids [1] have attracted considerable interest [2,3]. The model represents a distinct route to magnetic frustration on the honeycomb lattice, where each spin cannot simultaneously satisfy the bond-dependent and mutually orthogonal Ising interactions with its three neighbors. Realizing these interactions in crystalline materials involves a delicate balance [4–9] among the electron interaction, crystal-field splitting, and spin-orbit coupling. In particular, the desired Kitaev-type three-dimensional (3D) interaction anisotropy is at variance with the two-dimensional (2D) geometry of the honeycomb lattice. To best approximate the Kitaev model, the crystal-field and hopping parameters need to be locally restricted to the magnetic ions and their ligands, without significantly involving more distant atoms that reflect the lattice geometry.

Recently, cobalt oxides with a layered honeycomb-lattice structure, including $Na_2Co_2TeO_6$ (NCTO), $Na_3Co_2SbO_6$ (NCSO), and $BaCo_2(AsO_4)_2$ (BCAO), have been intensely studied for their potential to realize the Kitaev model [7,8,10–18]. Compared to the 4*d* and 5*d* counterparts such as in α-$RuCl_3$ [6] and Na_2IrO_3 [5], respectively, the Co^{2+} 3*d* orbitals in these compounds are expected to be more localized. However, whether this localization is sufficient to suppress direct (i.e., not via ligands) hopping between nearest neighbors and farther-neighbor hopping remains a point of contention [17,19–24]. While farther-neighbor hopping might be treated as a perturbation to the nearest-neighbor (Kitaev) model, which can already influence important characteristics of the magnetic order and excitations [18,22,25–27], direct hopping is believed to lead to a strong departure from the Kitaev model concerning the interaction anisotropy [17,19–21,23,24]. As most of the cobalt oxides do develop long-range magnetic order at low temperatures, such departures from the ideal Kitaev model cannot be neglected.

A crucial aspect related to the direct nearest-neighbor hopping, when combined with crystal-field and spin-orbit effects, is whether the cobalt oxides are better described by an easy-plane (XXZ) model than the Kitaev model. *Ab initio* calculations suggest that this may indeed be the case for NCTO and BCAO [19–21,23]. Yet, even for NCSO, which is considered more compatible with a Kitaev-like theoretical starting point [23,28,29], recent studies present evidence supporting XXZ-like anisotropy [30]. Notably, XXZ- and Kitaev-like models are very different in their magnetic frustration properties: A bond-independent XXZ model is bipartite on the honeycomb lattice, such that it needs to be supplemented by farther-neighbor interactions in order to be frustrated [19–21,24,31]. Even in the fully bond-dependent Ising limit, the frustration is still arguably weaker than in the Kitaev model, because the model no longer has three mutually orthogonal spin anisotropy axes (instead, they are 120° apart). It is thus important to search for signs of magnetic quantum fluctuations in the cobalt oxides to evaluate their potential for manifesting novel quantum states of matter.

In this paper, we present a comprehensive muon (μ^+)-spin relaxation (μSR) study of NCTO and NCSO, conducted from the paramagnetic states to deep inside their magnetically ordered states. By varying temperatures and applying

*miaoping@ihep.ac.cn
†yuan.li@pku.edu.cn

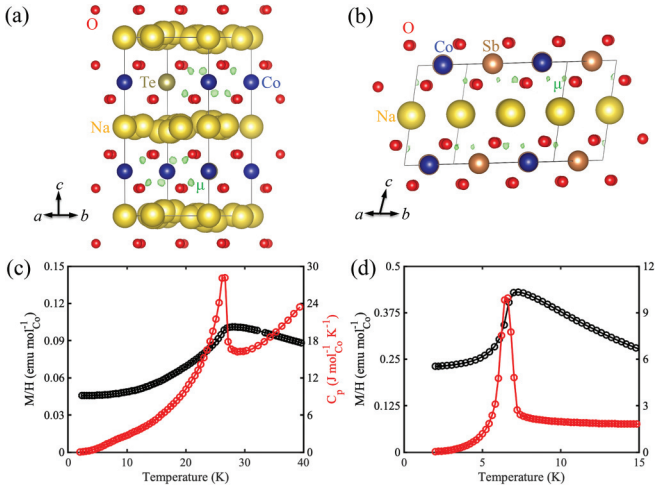

FIG. 1. (a), (b) Crystal structures of $Na_2Co_2TeO_6$ and $Na_3Co_2SbO_6$, respectively, along with calculated muon stoppage sites indicated by small spheres near the cobalt atoms. (c), (d) Magnetic susceptibility of $Na_2Co_2TeO_6$ and $Na_3Co_2SbO_6$, measured on single crystals with in-plane magnetic fields of 5000 and 1000 Oe, respectively. The data are plotted together with specific heat data measured in zero field to demonstrate T_N and the homogeneity of the samples.

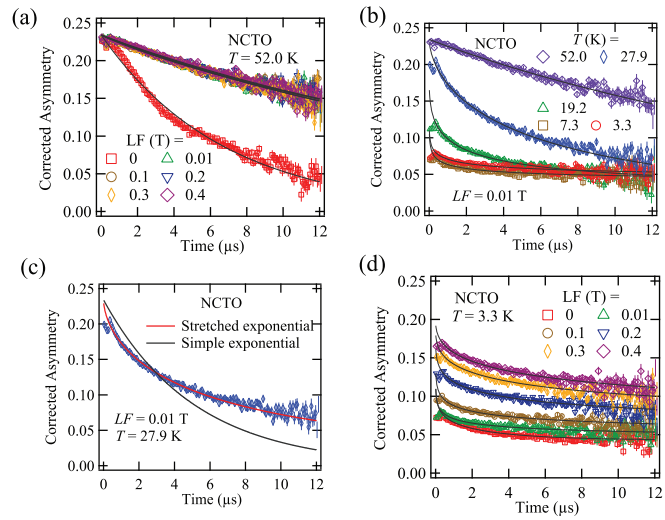

FIG. 2. (a) μSR spectra of NCTO measured far above T_N. A longitudinal field (LF) of 0.01 T decouples the nuclear dipolar fields. (b) Near-zero-field μSR spectra measured at selected temperatures. (c) Demonstration of stretched-exponential fitting of the data obtained in near-zero field and just above T_N. (d) Lowest-temperature spectra under various LFs, revealing a dual static and dynamic nature of the relaxation.

longitudinal magnetic fields, we were able to distinguish between muon-spin relaxation caused by static and dynamic magnetic moments. In both materials, we discovered that the dynamic relaxation rate peaks at a temperature substantially below the ordering temperature (T_N), displaying a stretched-exponential behavior indicative of a glasslike distribution of relaxation times. Crucially, we found that a considerable fraction of the spins maintain their dynamic nature even at temperatures that are an order of magnitude below T_N. These observations provide compelling evidence for significant quantum fluctuations in both systems, underscoring their highly frustrated nature. The persistent spin dynamics could also impose constraints on the nature of the magnetic ground states.

Figures 1(a) and 1(b) compare the crystal structures of NCTO and NCSO. The honeycomb-lattice cobalt layers are formed by edge-sharing CoO_6 octahedra. They are separated by sodium atoms and have weak interlayer magnetic coupling [25,32]. While this renders the difference in the interlayer stacking of the two systems (hexagonal in NCTO and monoclinic in NCSO) seemingly unimportant, the monoclinic distortion of NCSO affects the Co-O bonding geometry and produces dramatic in-plane magnetic anisotropy [33]. Both systems show large in-plane versus out-of-plane magnetization anisotropy [11,12,33], which can be attributed to either global XXZ-like easy-plane anisotropy, or bond-dependent Kitaev-like anisotropy supplemented by off-diagonal coupling [34]. Their transition temperatures T_N differ by about a factor of 4 [Figs. 1(c) and 1(d)], and it is believed that NCSO is closer to a ferromagnetic instability [10,33].

II. EXPERIMENTS

μSR is a powerful probe of both static and dynamic magnetization in solids. In both NCTO and NCSO, implanted muons are expected to stop not far from the cobalt layers [Figs. 1(a) and 1(b)], which makes them very sensitive to internal magnetic fields generated by the cobalt atoms. Our μSR experiments were performed on the ARTEMIS beam line at the Japan Proton Accelerator Research Complex (J-PARC), which utilizes both doublepulse higher-count-rate and single-pulse higher-time-resolution methods. Polycrystalline NCTO and NCSO were ground from single crystals grown with a self-flux method [12,33] and pressed into pellets of about 5 mm in thickness and 25 mm in diameter. NCTO was mounted in a helium-4 cryostat while NCSO was measured in both helium-4 and helium-3 cryostats. All the μSR data of NCSO discussed in the paper were from the helium-3 cryostat. The base temperatures of helium-4 and helium-3 cryostats are about 3.3 and 0.3 K, which are about one order of magnitude below the respective T_N of the systems. We performed our measurements under a variety of longitudinal magnetic fields (LFs, up to $H = 0.4$ T) parallel to the initial μ^+ spin direction, and analyzed the data using the software suite MUSRFIT [35]. μSR spectra are represented by the corrected asymmetry of the muon-decay counts as a function of delay time after implantation.

III. RESULTS

Figure 2(a) displays the μSR spectra of NCTO obtained at 52 K. As the temperature is far above $T_N = 26.7$ K, the observed relaxation is not caused by static internal fields related to the magnetic order. The significant difference between the zero-field (ZF) and the LF = 0.01 T spectra indicates that the former is affected by cobalt nuclear magnetic moments, which the weak LF is sufficient to decouple. As such a weak LF is not expected to be comparable to internal magnetic fields generated by the Co electronic magnetic moments (over $2\mu_B$

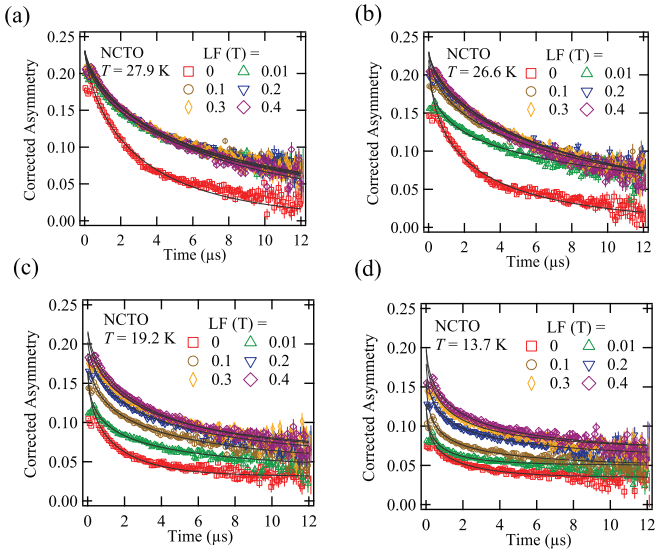

FIG. 3. μSR spectra of $Na_2Co_2TeO_6$ (NCTO) under various longitudinal fields (LFs) at (a) $T = 27.9$ K, (b) 26.6 K, (c) 19.2 K, and (d) 13.7 K.

in NCTO [12]), we continue to display in Fig. 2(b) the spectra obtained with LF = 0.01 T at lower temperatures. Additional temperature- and LF-dependent data of NCTO are displayed in Fig. 3, and similarly obtained data for NCSO are displayed in Figs. 4 and 5.

For a quantitative analysis, we fit the spectra to a sum of dynamic and static components [36,37],

$$A_0 P_z(H,t) = A_{bg} + A_1 \exp[-(\Lambda t)^{\beta}] + A_2\{\alpha(H)\exp[-(\lambda_L t)] + [1-\alpha(H)]\cos(\gamma_\mu B t + \phi)\exp[-(\lambda_T t)]\}, \quad (1)$$

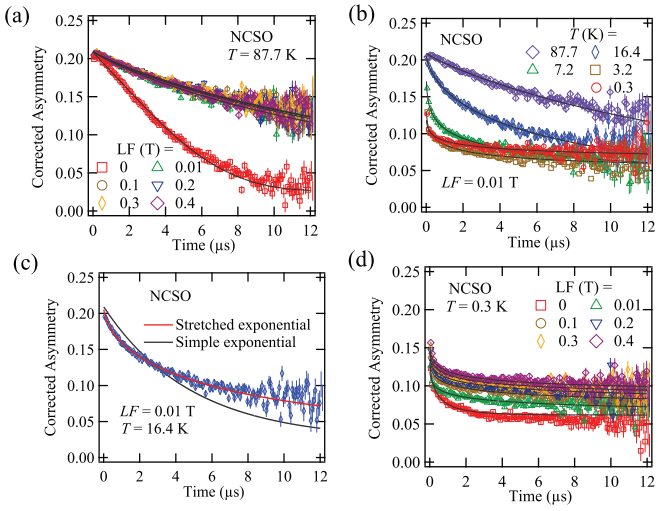

FIG. 4. (a) μSR spectra of $Na_3Co_2SbO_6$ (NCSO) measured far above T_N. A longitudinal field (LF) of 0.01 T decouples the nuclear dipolar fields. (b) Near-zero-field μSR spectra measured at selected temperatures. (c) Demonstration of stretched-exponential fitting of the data obtained in near-zero field and just above T_N. (d) Lowest-temperature spectra under various LFs, revealing a dual static and dynamic nature of the relaxation.

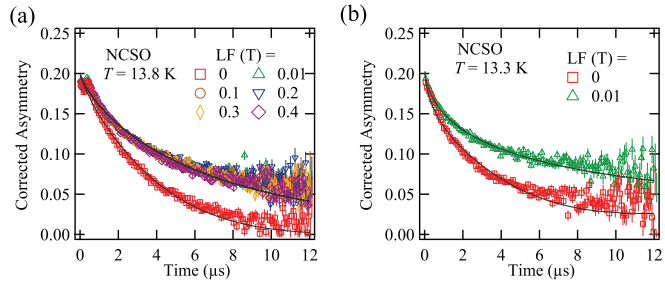

FIG. 5. μSR spectra of NCSO measured using (a) the helium-4 cryostat and (b) the helium-3 cryostat. The ZF spectra clearly show that the background level for the helium-4 cryostat is negligible and that for the helium-3 cryostat is about 0.025. All the μSR data of NCSO discussed in the paper were measured by the helium-3 cryostat except for that in (a).

where A_0 is the initial asymmetry and $P_z(H,t)$ the normalized polarization function. A_1 and A_2 are magnitudes of contributions from the dynamic and static phases, respectively, and A_{bg} denotes the background asymmetry. A_{bg} is negligible for NCTO and determined to be 0.025 for NCSO, as shown by the ZF spectra at 26.6 and 13.3 K in Figs. 3 and 5, respectively. The dynamic contribution is best described by a stretched-exponential relaxation function, where Λ is the dynamic spin-lattice-relaxation rate and β the exponent, the physical meaning of which will be discussed later. A_2 is zero above T_N and increases (at the cost of decreasing A_1) below T_N. α accounts for the effect of LFs on the relaxation caused by the magnetic order. Because of powder average, α equals 1/3 at LF = 0.01 T (or ZF) and gradually increases with increasing LFs. This is manifested by the fact that the data in Figs. 2(d) and 4(d) for LF above 0.01 T are approximately offset from one another along the vertical direction. The oscillation term $\cos(\gamma_\mu B t + \phi)$ is practically unimportant in our measurements due to the fast damping rate of the oscillations (λ_T) [38] and our limited time resolution. The relaxation rate λ_L is practically negligible at low temperatures because the spectra at LF = 0.01 T are virtually time independent at large t [Figs. 2(b) and 4(b)].

Figure 6 summarizes our findings from the fits for both NCTO and NCSO. At LF = 0.01 T, we observe a clear decrease in the initial asymmetry (corrected asymmetry at $t = 0$) upon cooling below T_N as the long-range magnetic order forms [Fig. 6(a)]. This can be directly seen from Fig. 2(b), where each of the five spectra starts from a different initial value. We attribute this behavior to the fact that the internal magnetic fields associated with the static phase [A_2 term in Eq. (1)] are strong, making the asymmetry oscillate too rapidly to be resolved by our time resolution. Our understanding about this static-phase contribution is corroborated by the spectra under LFs at 3.3 K [Fig. 2(d)], where the initial asymmetry increases with increasing LFs. Especially for NCTO, the observed initial asymmetry does not behave as a typical order parameter below T_N. Instead, it undergoes a gradual, nearly linear decrease with cooling at LF = 0.01 T, and levels off below about 16 K [Fig. 6(a)]. This indicates that the system somehow resists to develop conventional long-range

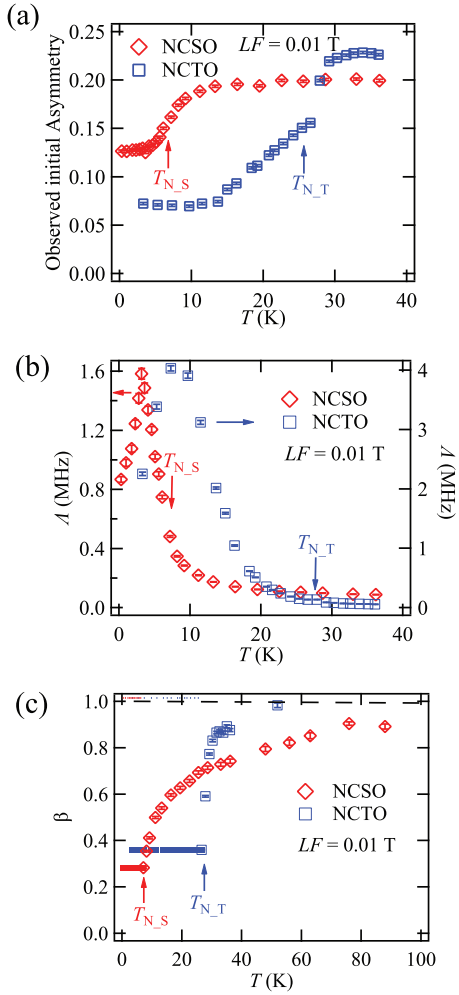

FIG. 6. (a) Muon-spin asymmetry in the nominal $t = 0$ limit measured by our relatively poor time resolution. (b) Muon relaxation rate as a function of temperature. The relaxation is primarily caused by dynamic internal fields because longitudinal fields up to 0.4 T have little effect on it [Fig. 2(d)]. (c) Stretched exponent used in our fits to the time spectra (see text). Below T_N, the data are consistent with a stable exponent and are therefore fit to a common value. Arrows indicate T_N of the two systems.

order, possibly due to magnetic frustration and the existence of closely competing ground states.

After the initial decrease in asymmetry, the spectra in Fig. 2(b) show gradual damping over time, which is observed even under LF = 0.4 T at 3.3 K [Fig. 2(d)], indicating that a dynamic phase coexists with the static phase. This dynamic contribution is characterized by the relaxation rate Λ and the stretched exponent β [A_1 term in Eq. (1)]. It is clear from Fig. 2(c) that a simple exponential function, i.e., with $\beta = 1$, would fail to describe the data obtained near T_N. Instead, we find that β decreases from 1 steeply to about 1/3 as the sample is cooled towards T_N, and stays that way below T_N [Fig. 6(c)]. Significant deviations from a simple exponential relaxation function usually signify a broad distribution of spatially inhomogeneous correlation times, which is commonly observed in glassy magnets [39–41]. Indeed, $\beta = 1/3$ has been reported in the metallic spin glass AgMn [42,43]. Since NCTO and

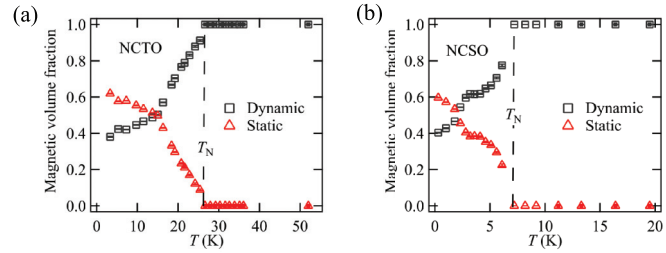

FIG. 7. Volume fraction of dynamic $[A_1/(A_1 + A_2)]$ and static phases $[A_2/(A_1 + A_2)]$ as determined from the fit values of A_1 and A_2 according to Eq. (1). $A_2 = 0$ has been assumed in the fits above T_N.

NCSO are chemically ordered systems, we attribute our observation of stretched exponents to spin-glass-like behaviors which have previously been observed in geometrically frustrated antiferromagnets [44–46]. This understanding is further supported by the unusual temperature evolution of the relaxation rate Λ, which serves as a one-parameter abstraction of the relaxation process. Namely, we find that Λ reaches its maximum only at a temperature significantly lower than T_N [Fig. 6(b)], which is inconsistent with a conventional second-order phase transition at T_N [40,47]. We notice that NCTO undergoes successive magnetic transitions below T_N [15,48,49] while NCSO exhibits no further magnetic transition below T_N [33]. The data suggest that substantial spin fluctuations continue to exist below T_N until a much lower temperature is reached. This is consistent with previous inelastic neutron scattering results on NCTO [32], where spectrally well-defined spin waves were only observed far below T_N.

IV. DISCUSSION

Taken together, our μSR data indicate that the magnetic orders in NCTO and NCSO are distinct from conventional long-range magnetic order [50], as they (1) are not accompanied by an anomaly of Λ at T_N [Fig. 6(b)], (2) exhibit a "glassy" growth of the internal fields below T_N [Fig. 6(a)], and (3) have a wide distribution of correlation times even in the well-ordered state [Fig. 6(c)]. To go one step further, we can use A_1 and A_2 in Eq. (1) to estimate the volume fractions that are dynamic and static, respectively, at a given temperature (Fig. 7). In line with the unconventional nature of the orders, the result reveals that a significant fraction of the samples remains dynamic down to the lowest temperature. In fact, despite the different T_N, the two systems look remarkably similar. In the case of NCTO, it is known that the spin excitation spectrum exhibits a gap of over 1 meV at 3.3 K [15,25,32], which makes thermal fluctuations unable to cause significant spin dynamics in the system. Because NCSO exhibits even stronger spin anisotropy than NCTO [33], it is likely that in the well-ordered state the system has an even larger excitation gap than NCTO. However, our data show that the dynamic volume fraction in NCSO is as large as 40% even at the very low temperature of 0.3 K. We therefore believe that the observed spin dynamics are caused by quantum rather than thermal fluctuations.

It is also important to consider the role of quenched disorders, which have been shown to affect spin dynamics

observed by μSR in related systems such as α-$RuCl_3$ and Cu_2IrO_3 [51–54]. Having examined our crystals with scanning transmission electron microscopy, in the search for lattice imperfections similar to those in Cu_2IrO_3 [53], we confirm that both NCTO and NCSO have well-ordered crystal lattices without frequent stacking faults or pronounced chemical inhomogeneity. While our μSR data were taken on polycrystalline samples, the samples were obtained by grinding single crystals which have previously been shown to be of very high quality and homogeneity [12,32,33]. We further note that a recent μSR study of single-crystalline NCTO has arrived at similar conclusions as ours [38]. Therefore, we believe that disorders are weak in our samples and cannot explain the observed persisting dynamics down to very low temperatures.

The presence of significant spin dynamics in both NCTO and NCSO deep in the ordered state suggests that the systems may be driven into a quantum paramagnetic state if the semiclassical order can be suppressed. Coexisting long-range order and fractionalized excitations have been proposed in a recent thermal transport study [55]. We further speculate that the dynamic phase volumes, up to about 40% in both systems at the lowest temperature, may corroborate recent proposals of multi-**q** magnetic orders in the two systems [30,32,48,49,56]. Specifically, if the spin anisotropy of these cobalt oxides is indeed XXZ- rather than Kitaev-like [17,19–21,23,24], meaning that the ordered moments all lie parallel to the *ab* plane [30], the proposed multi-**q** orders would feature 1/4 of the cobalt sites being (classically) "spinless" (in spite of large ordered moment size measured in diffraction [57,58]) in NCTO [32,48,49] and half of the sites having smaller classical moments than the other half [30]. Such scenarios are in good qualitative agreement with the dynamic volume fractions we observe.

V. CONCLUSION

To conclude, we have discovered persistent and spatially inhomogeneous spin dynamics deep inside the magnetically ordered states of two layered honeycomb-lattice cobalt oxides. Our findings indicate that the systems are highly frustrated despite their formation of long-range order, and imply that they continue to hold promise for realizing different quantum states of matter if the semiclassical aspect of the ground states can be further suppressed.

ACKNOWLEDGEMENTS

We are grateful for technical support for calculation of muon stoppage sites by Dr. H. Li. The work was supported by the National Basic Research Program of China (Grant No. 2021YFA1401900), the NSF of China (Grants No. 12061131004, No. 11888101, No. 12005243, and No. 22205239), and the Guangdong Basic and Applied Basic Research Foundation (Grants No. 2022B1515120014, No. 2023B0303000003 and No. 2023B1515120060). The μSR experiments were performed at the MLF, J-PARC, Japan, under a user program (Grants No. 2019B0201 and No. 2022A0141).

[1] A. Kitaev, Anyons in an exactly solved model and beyond, Ann. Phys. **321**, 2 (2006).
[2] H. Takagi, T. Takayama, G. Jackeli, G. Khaliullin, and S. E. Nagler, Concept and realization of Kitaev quantum spin liquids, Nat. Rev. Phys. **1**, 264 (2019).
[3] S. Trebst and C. Hickey, Kitaev materials, Phys. Rep. **950**, 1 (2022).
[4] G. Jackeli and G. Khaliullin, Mott insulators in the strong spin-orbit coupling limit: From Heisenberg to a quantum compass and Kitaev models, Phys. Rev. Lett. **102**, 017205 (2009).
[5] J. Chaloupka, G. Jackeli, and G. Khaliullin, Kitaev-Heisenberg model on a honeycomb lattice: Possible exotic phases in iridium oxides A_2IrO_3, Phys. Rev. Lett. **105**, 027204 (2010).
[6] K. W. Plumb, J. P. Clancy, L. J. Sandilands, V. V. Shankar, Y. F. Hu, K. S. Burch, H.-Y. Kee, and Y.-J. Kim, α-$RuCl_3$: A spin-orbit assisted Mott insulator on a honeycomb lattice, Phys. Rev. B **90**, 041112(R) (2014).
[7] H. Liu and G. Khaliullin, Pseudospin exchange interactions in d^7 cobalt compounds: Possible realization of the Kitaev model, Phys. Rev. B **97**, 014407 (2018).
[8] R. Sano, Y. Kato, and Y. Motome, Kitaev-Heisenberg Hamiltonian for high-spin d^7 Mott insulators, Phys. Rev. B **97**, 014408 (2018).
[9] Y. Motome, R. Sano, S. Jang, Y. Sugita, and Y. Kato, Materials design of Kitaev spin liquids beyond the Jackeli–Khaliullin mechanism, J. Phys.: Condens. Matter **32**, 404001 (2020).
[10] H. Liu, J. Chaloupka, and G. Khaliullin, Kitaev spin liquid in 3*d* transition metal compounds, Phys. Rev. Lett. **125**, 047201 (2020).
[11] J.-Q. Yan, S. Okamoto, Y. Wu, Q. Zheng, H. D. Zhou, H. B. Cao, and M. A. McGuire, Magnetic order in single crystals of $Na_3Co_2SbO_6$ with a honeycomb arrangement of $3d^7$ Co^{2+} ions, Phys. Rev. Mater. **3**, 074405 (2019).
[12] W. Yao and Y. Li, Ferrimagnetism and anisotropic phase tunability by magnetic fields in $Na_2Co_2TeO_6$, Phys. Rev. B **101**, 085120 (2020).
[13] R. Zhong, T. Gao, N. P. Ong, and R. J. Cava, Weak-field induced nonmagnetic state in a Co-based honeycomb, Sci. Adv. **6**, eaay6953 (2020).
[14] M. Songvilay, J. Robert, S. Petit, J. A. Rodriguez-Rivera, W. D. Ratcliff, F. Damay, V. Balédent, M. Jiménez-Ruiz, P. Lejay, E. Pachoud, A. Hadj-Azzem, V. Simonet, and C. Stock, Kitaev interactions in the Co honeycomb antiferromagnets $Na_3Co_2SbO_6$ and $Na_2Co_2TeO_6$, Phys. Rev. B **102**, 224429 (2020).
[15] G. Lin, J. Jeong, C. Kim, Y. Wang, Q. Huang, T. Masuda, S. Asai, S. Itoh, G. Günther, M. Russina, Z. Lu, J. Sheng, L. Wang, J. Wang, G. Wang, Q. Ren, C. Xi, W. Tong, L. Ling, Z. Liu *et al.*, Field-induced quantum spin disordered state in spin-1/2 honeycomb magnet $Na_2Co_2TeO_6$, Nat. Commun. **12**, 5559 (2021).
[16] C. Kim, J. Jeong, G. Lin, P. Park, T. Masuda, S. Asai, S. Itoh, H.-S. Kim, H. Zhou, J. Ma, and J.-G. Park, Antiferromagnetic Kitaev interaction $J_{\text{eff}} = 1/2$ cobalt honeycomb materials

$Na_3Co_2SbO_6$ and $Na_2Co_2TeO_6$, J. Phys.: Condens. Matter **34**, 045802 (2022).

[17] C. Kim, H.-S. Kim, and J.-G. Park, Spin-orbital entangled state and realization of Kitaev physics in 3*d* cobalt compounds: a progress report, J. Phys.: Condens. Matter **34**, 023001 (2022).

[18] A. L. Sanders, R. A. Mole, J. Liu, A. J. Brown, D. Yu, C. D. Ling, and S. Rachel, Dominant Kitaev interactions in the honeycomb materials $Na_3Co_2SbO_6$ and $Na_2Co_2TeO_6$, Phys. Rev. B **106**, 014413 (2022).

[19] S. Das, S. Voleti, T. Saha-Dasgupta, and A. Paramekanti, XY magnetism, Kitaev exchange, and long-range frustration in the $J_{\text{eff}} = \frac{1}{2}$ honeycomb cobaltates, Phys. Rev. B **104**, 134425 (2021).

[20] P. A. Maksimov, A. V. Ushakov, Z. V. Pchelkina, Y. Li, S. M. Winter, and S. V. Streltsov, *Ab initio* guided minimal model for the "Kitaev" material $BaCo_2(AsO_4)_2$: Importance of direct hopping, third-neighbor exchange, and quantum fluctuations, Phys. Rev. B **106**, 165131 (2022).

[21] S. M. Winter, Magnetic couplings in edge-sharing high-spin d^7 compounds, J. Phys.: Mater. **5**, 045003 (2022).

[22] S. K. Pandey and J. Feng, Spin interaction and magnetism in cobaltate Kitaev candidate materials: An *ab initio* and model Hamiltonian approach, Phys. Rev. B **106**, 174411 (2022).

[23] X. Liu and H.-Y. Kee, Non-Kitaev versus Kitaev honeycomb cobaltates, Phys. Rev. B **107**, 054420 (2023).

[24] T. Halloran, F. Desrochers, E. Z. Zhang, T. Chen, L. E. Chern, Z. Xu, B. Winn, M. Graves-Brook, M. B. Stone, A. I. Kolesnikov, Y. Qiu, R. Zhong, R. Cava, Y. B. Kim, and C. Broholm, Geometrical frustration versus Kitaev interactions in $BaCo_2(AsO_4)_2$, Proc. Natl. Acad. Sci. USA **120**, e2215509119 (2023).

[25] W. Yao, K. Iida, K. Kamazawa, and Y. Li, Excitations in the ordered and paramagnetic states of honeycomb magnet $Na_2Co_2TeO_6$, Phys. Rev. Lett. **129**, 147202 (2022).

[26] W. G. F. Krüger, W. Chen, X. Jin, Y. Li, and L. Janssen, Triple-q order in $Na_2Co_2TeO_6$ from proximity to hidden-SU(2)-symmetric point, Phys. Rev. Lett. **131**, 146702 (2023).

[27] J. Wang and Z.-X. Liu, Effect of ring-exchange interactions in the extended Kitaev honeycomb model, Phys. Rev. B **108**, 014437 (2023).

[28] E. Vavilova, T. Vasilchikova, A. Vasiliev, D. Mikhailova, V. Nalbandyan, E. Zvereva, and S. V. Streltsov, Magnetic phase diagram and possible Kitaev-like behavior of the honeycomb-lattice antimonate $Na_3Co_2SbO_6$, Phys. Rev. B **107**, 054411 (2023).

[29] B. Kang, M. Park, S. Song, S. Noh, D. Choe, M. Kong, M. Kim, C. Seo, E. K. Ko, G. Yi, J.-W. Yoo, S. Park, J. M. Ok, and C. Sohn, Honeycomb oxide heterostructure as a candidate host for a Kitaev quantum spin liquid, Phys. Rev. B **107**, 075103 (2023).

[30] Y. Gu, X. Li, Y. Chen, K. Iida, A. Nakao, K. Munakata, V. O. Garlea, Y. Li, G. Deng, I. A. Zaliznyak, J. M. Tranquada, and Y. Li, In-plane multi-q magnetic ground state of $Na_3Co_2CbO_6$, Phys. Rev. B **109**, L060410 (2024).

[31] H. S. Nair, J. M. Brown, E. Coldren, G. Hester, M. P. Gelfand, A. Podlesnyak, Q. Huang, and K. A. Ross, Short-range order in the quantum XXZ honeycomb lattice material $BaCo_2(PO_4)_2$, Phys. Rev. B **97**, 134409 (2018).

[32] W. Chen, X. Li, Z. Hu, Z. Hu, L. Yue, R. Sutarto, F. He, K. Iida, K. Kamazawa, W. Yu, X. Lin, and Y. Li, Spin-orbit phase behavior of $Na_2Co_2TeO_6$ at low temperatures, Phys. Rev. B **103**, L180404 (2021).

[33] X. Li, Y. Gu, Y. Chen, V. O. Garlea, K. Iida, K. Kamazawa, Y. Li, G. Deng, Q. Xiao, X. Zheng, Z. Ye, Y. Peng, I. A. Zaliznyak, J. M. Tranquada, and Y. Li, Giant magnetic in-plane anisotropy and competing instabilities in $Na_3Co_2SbO_6$, Phys. Rev. X **12**, 041024 (2022).

[34] L. Janssen, E. C. Andrade, and M. Vojta, Magnetization processes of zigzag states on the honeycomb lattice: Identifying spin models for α-$RuCl_3$ and Na_2IrO_3, Phys. Rev. B **96**, 064430 (2017).

[35] A. Suter and B. M. Wojek, MUSRFIT: A free platform-independent framework for μSR data analysis, Phys. Procedia **30**, 69 (2012).

[36] H. S. Jeevan, D. T. Adroja, A. D. Hillier, Z. Hossain, C. Ritter, and C. Geibel, Muon spin relaxation and neutron diffraction investigations of quadrupolar and magnetically ordered states of $YbRu_2Ge_2$, Phys. Rev. B **84**, 184405 (2011).

[37] M. Kundu, S. Pakhira, R. Choudhary, D. Paudyal, N. Lakshminarasimhan, M. Avdeev, S. Cottrell, D. Adroja, R. Ranganathan, and C. Mazumdar, Complex magnetic properties associated with competing local and itinerant magnetism in $Pr_2Co_{0.86}Si_{2.88}$, Sci. Rep. **11**, 13245 (2021).

[38] G. Lin, J. Jiao, X. Li, M. Shu, O. Zaharko, T. Shiroka, T. Hong, A. I. Kolesnikov, G. Deng, S. Dunsiger, H. Zhou, T. Shang, and J. Ma, Static magnetic order with strong quantum fluctuations in spin-1/2 honeycomb magnet $Na_2Co_2TeO_6$, arXiv:2312.06284.

[39] Y. J. Uemura, T. Yamazaki, D. R. Harshman, M. Senba, and E. J. Ansaldo, Muon-spin relaxation in AuFe and CuMn spin glasses, Phys. Rev. B **31**, 546 (1985).

[40] R. H. Heffner, L. P. Le, M. F. Hundley, J. J. Neumeier, G. M. Luke, K. Kojima, B. Nachumi, Y. J. Uemura, D. E. MacLaughlin, and S. W. Cheong, Ferromagnetic ordering and unusual magnetic ion dynamics in $La_{0.67}Ca_{0.33}MnO_3$, Phys. Rev. Lett. **77**, 1869 (1996).

[41] P. Miao, R. Wang, W. Zhu, J. Liu, T. Liu, J. Hu, S. Li, Z. Tan, A. Koda, F. Zhu, E. Feng, Y. Su, T. Kamiyama, Y. Xiao, and F. Pan, Revealing magnetic ground state of a layered cathode material by muon spin relaxation and neutron scattering experiments, Appl. Phys. Lett. **114**, 203901 (2019).

[42] I. A. Campbell, A. Amato, F. N. Gygax, D. Herlach, A. Schenck, R. Cywinski, and S. H. Kilcoyne, Dynamics in canonical spin glasses observed by muon spin depolarization, Phys. Rev. Lett. **72**, 1291 (1994).

[43] A. Keren, P. Mendels, I. A. Campbell, and J. Lord, Probing the spin-spin dynamical autocorrelation function in a spin glass above T_g via muon spin relaxation, Phys. Rev. Lett. **77**, 1386 (1996).

[44] S. R. Dunsiger, R. F. Kiefl, K. H. Chow, B. D. Gaulin, M. J. P. Gingras, J. E. Greedan, A. Keren, K. Kojima, G. M. Luke, W. A. MacFarlane, N. P. Raju, J. E. Sonier, Y. J. Uemura, and W. D. Wu, Low temperature spin dynamics of geometrically frustrated antiferromagnets $Y_2Mo_2O_7$ and $Y_2Mo_{1.6}Ti_{0.4}O_7$ studied by muon spin relaxation, J. Appl. Phys. **79**, 6636 (1996).

[45] J. S. Gardner, B. D. Gaulin, S.-H. Lee, C. Broholm, N. P. Raju, and J. E. Greedan, Glassy statics and dynamics in the chemically ordered pyrochlore antiferromagnet $Y_2Mo_2O_7$, Phys. Rev. Lett. **83**, 211 (1999).

[46] S. K. Dey, K. Ishida, H. Okabe, M. Hiraishi, A. Koda, T. Honda, J. Yamaura, H. Kageyama, and R. Kadono, Local spin dynamics in the geometrically frustrated Mo pyrochlore antiferromagnet $Lu_2Mo_2O_{5-y}N_2$, Phys. Rev. B **107**, 024407 (2023).

[47] P. C. M. Gubbens, A. A. Moolenaar, P. Dalmas De Réotier, A. Yaouanc, F. Kayzel, J. J. M. Franse, K. Prokes, C. E. Snel, P. Bonville, J. A. Hodges, P. Imbert, and P. Pari, Spin dynamics in $RENi_5$ ferromagnets by μSR measurements, Hyperfine Interact. **85**, 239 (1994).

[48] C. H. Lee, S. Lee, Y. S. Choi, Z. H. Jang, R. Kalaivanan, R. Sankar, and K.-Y. Choi, Multistage development of anisotropic magnetic correlations in the Co-based honeycomb lattice $Na_2Co_2TeO_6$, Phys. Rev. B **103**, 214447 (2021).

[49] J. Kikuchi, T. Kamoda, N. Mera, Y. Takahashi, K. Okumura, and Y. Yasui, Field evolution of magnetic phases and spin dynamics in the honeycomb lattice magnet $Na_2Co_2TeO_6$: ^{23}Na NMR study, Phys. Rev. B **106**, 224416 (2022).

[50] P. Miao, Z. Tan, S. Lee, Y. Ishikawa, S. Torii, M. Yonemura, A. Koda, K. Komatsu, S. Machida, A. Sano-Furukawa, T. Hattori, X. Lin, K. Li, T. Mochiku, R. Kikuchi, C. Kawashima, H. Takahashi, Q. Huang, S. Itoh, R. Kadono *et al.*, Origin of magnetovolume effect in a cobaltite, Phys. Rev. B **103**, 094302 (2021).

[51] F. Lang, P. J. Baker, A. A. Haghighirad, Y. Li, D. Prabhakaran, R. Valentí, and S. J. Blundell, Unconventional magnetism on a honeycomb lattice in α-$RuCl_3$ studied by muon spin rotation, Phys. Rev. B **94**, 020407(R) (2016).

[52] I. Yamauchi, M. Hiraishi, H. Okabe, S. Takeshita, A. Koda, K. M. Kojima, R. Kadono, and H. Tanaka, Local spin structure of the α-$RuCl_3$ honeycomb-lattice magnet observed via muon spin rotation/relaxation, Phys. Rev. B **97**, 134410 (2018).

[53] E. M. Kenney, C. U. Segre, W. Lafargue-Dit-Hauret, O. I. Lebedev, M. Abramchuk, A. Berlie, S. P. Cottrell, G. Simutis, F. Bahrami, N. E. Mordvinova, G. Fabbris, J. L. McChesney, D. Haskel, X. Rocquefelte, M. J. Graf, and F. Tafti, Coexistence of static and dynamic magnetism in the Kitaev spin liquid material Cu_2IrO_3, Phys. Rev. B **100**, 094418 (2019).

[54] Y. S. Choi, C. H. Lee, S. Lee, S. Yoon, W.-J. Lee, J. Park, A. Ali, Y. Singh, J.-C. Orain, G. Kim, J.-S. Rhyee, W.-T. Chen, F. Chou, and K.-Y. Choi, Exotic low-energy excitations emergent in the random Kitaev magnet Cu_2IrO_3, Phys. Rev. Lett. **122**, 167202 (2019).

[55] S. Guang, N. Li, R. L. Luo, Q. Huang, Y. Wang, X. Yue, K. Xia, Q. Li, X. Zhao, G. Chen, H. Zhou, and X. Sun, Thermal transport of fractionalized antiferromagnetic and field-induced states in the Kitaev material $Na_2Co_2TeO_6$, Phys. Rev. B **107**, 184423 (2023).

[56] W. Yao, Y. Zhao, Y. Qiu, C. Balz, J. R. Stewart, J. W. Lynn, and Y. Li, Magnetic ground state of the Kitaev $Na_2Co_2TeO_6$ spin liquid candidate, Phys. Rev. Res. **5**, L022045 (2023).

[57] E. Lefrançois, M. Songvilay, J. Robert, G. Nataf, E. Jordan, L. Chaix, C. V. Colin, P. Lejay, A. Hadj-Azzem, R. Ballou, and V. Simonet, Magnetic properties of the honeycomb oxide $Na_2Co_2TeO_6$, Phys. Rev. B **94**, 214416 (2016).

[58] A. K. Bera, S. M. Yusuf, A. Kumar, and C. Ritter, Zigzag antiferromagnetic ground state with anisotropic correlation lengths in the quasi-two-dimensional honeycomb lattice compound $Na_2Co_2TeO_6$, Phys. Rev. B **95**, 094424 (2017).